Effect of Nonionic Admixtures on the Adsorption of Ionic Surfactants at Fluid Interfaces. 2. Sodium Dodecylbenzene Sulfonate and Dodecylbenzene

K. D. Danov,[†] S. D. Kralchevska,[†] P. A. Kralchevsky,*[,†] G. Broze,[‡] and A. Mehreteab[§]

Laboratory of Chemical Physics & Engineering, Faculty of Chemistry, University of Sofia, 1164 Sofia, Bulgaria, Colgate-Palmolive R&D, Inc., Avenue du Parc Industriel, B-4041 Milmort (Herstal), Belgium, and Colgate-Palmolive Technology Center, Piscataway, New Jersey 08854-5596

Received November 14, 2002. In Final Form: April 9, 2003

Equilibrium surface tension isotherms of sodium dodecylbenzene sulfonate (DDBS) are obtained at various fixed concentrations of NaCl. The contents of unsulfonated dodecylbenzene (DDB) in the used surfactant sample is determined by processing the surface-tension data. Having determined the parameters of the best fit, we computed the adsorption of surfactants (anionic DDBS and nonionic DDB), the binding of counterions in the Stern layer, the surface electric potential, the surface elasticity, etc., each of them for various surfactant and salt concentrations. The results show that for the solutions without added NaCl, the adsorption layer consists mostly of the nonionic DDB, irrespective of its small mole fraction in the surfactant blend. The admixture of DDB in the sample of DDBS leads to a significant increase of the surface elasticity. Moreover, even minimal added amounts of $CrCl_3$ or $Fe_2(SO_4)_3$ cause a considerable reduction in the surface tension, which is due to the greater binding energies of some of the counterions released by the latter electrolytes. The paper gives a quantitative analysis and description of the adsorption from aqueous solutions of a technical ionic surfactant. The followed strategy, which was to determine the contents of the admixtures and to account for their presence in the theoretical model, rather than to purify the surfactant, may find applications to other mixed surfactant systems.

1. Introduction

The recent advance in the field of adsorption of ionic surfactants at fluid interfaces, including the account for the electric double layer and the counterion binding, was reviewed in refs 1−4, as well as in the first part of the present series, ref 5. In the latter paper, we developed a theoretical method for determining small contents of dodecanol in samples of sodium dodecyl sulfate (SDS) by a detailed analysis of surface-tension isotherms. As a tool for our analysis, we employed the van der Waals model. Its application to data for alkanols and anionic surfactants gave an excluded area per adsorbed molecule equal to the geometrical area of the molecular cross section and adsorption energies consonant with the Traube rule. Knowing the parameters of the model, we computed various properties of the surfactant adsorption layer: adsorption of the surfactant species, occupancy of the Stern layer by bound counterions, surface electric potential, surface dilatational (Gibbs) elasticity, and so forth. The calculated adsorptions of SDS are in agreement with results of direct experimental methods.[6] The surface potential and the Gibbs elasticity, determined from the fits of surface tension isotherms, can be further used to predict the equilibrium thickness of foam and emulsion films and to analyze their stability. Moreover, the knowledge of the equilibrium properties of the surfactant adsorption layer is a prerequisite for a quantitative description of the dynamic interfacial tension.[7]

In brief, the analysis of surface tension isotherms by means of an adequate model can be used as a quantitative method for a complete characterization of surfactant adsorption layers. With this end in view, we undertook surface-tension measurements with the anionic surfactant sodium dodecylbenzene sulfonate (DDBS), which are described in the present paper. DDBS is a typical representative of the linear alkylbenzene sulfonates (LAS). The latter is the world's largest volume synthetic surfactant and is widely used in household detergents as well as in numerous industrial applications. It was developed as a biodegradable replacement for nonlinear (branched) alkylbenzene sulfonate.[8] Due to the specific production procedure, the samples of DDBS commonly contain an admixture of Na_2SO_4, which can be quantified by electroconductivity measurements; see section 2.2.

Our first attempt to interpret the experimental surface tension isotherms of DDBS solutions showed an enormous discrepancy between the experimental data and the theoretical model from ref 9, which had been found to excellently work for SDS solutions[6] (see section 2.3). Our

* To whom correspondence should be addressed. Fax: 359-2-962-5643. E-mail: pk@lcpe.uni-sofia.bg.

[†] University of Sofia.

[‡] Colgate-Palmolive R&D, Inc.

[§] Colgate-Palmolive Technology Center.

(1) Prosser, A. J.; Franses, E. I. *Colloids Surf., A* **2001**, *178*, 1.

(2) Fainerman, V. B.; Lucassen-Reynders, E. H. *Adv. Colloid Interface Sci.* **2002**, *96*, 295.

(3) Fainerman, V. B.; Möbius, D.; Miller, R. *Surfactants*: *Chemistry, Interfacial Properties, Applications*; Elsevier: Amsterdam, 2001.

(4) Kralchevsky, P. A.; Nagayama, K. *Particles at Fluid Interfaces and Membranes*; Elsevier: Amsterdam, 2001; Chapter 1.

(5) Kralchevsky, P. A.; Danov, K. D.; Kolev, V. L.; Broze, G.; Mehreteab, A. *Langmuir* **2003**, *19*, 5004.

(6) Kolev, V. L.; Danov, K. D.; Kralchevsky, P. A.; Broze, G.; Mehreteab, A. *Langmuir* **2002**, *18*, 9106.

(7) Danov, K. D.; Kolev, V. L.; Kralchevsky, P. A.; Broze, G.; Mehreteab, A. *Langmuir* **2000**, *16*, 2942.

(8) Modler, R. F.; Willhalm, R.; Yoshida, Y. *Linear Alkylate Sulfonates, Chemical Economics Handbook*; SRI International: Menlo Park, CA, 1998.

(9) Kralchevsky, P. A.; Danov, K. D.; Broze, G.; Mehreteab, A. *Langmuir* **1999**, *15*, 2351.

10.1021/la0268505 CCC: $25.00 © 2003 American Chemical Society
Published on Web 05/15/2003

first guess about the reason for the observed discrepancy was that it can be due to the presence of minor impurities of ions, such as Cr^{3+} and Fe^{3+}, which strongly bind in the Stern layer and can affect the solution's surface tension (see section 5 below). However, the chemical analysis of the used surfactant sample and deionized water showed that the amount of such admixtures is negligible. Then, we took into account the fact that the commercially available samples of DDBS commonly contain some amount of unsulfonated dodecylbenzene (DDB). As a result, we achieved an excellent agreement between theory and experiment and determined the content of DDB in the used DDBS from the best fit of the data.

The experimental data (see below) indicate that the presence of DDB in a sample of DDBS leads to a considerable decrease in the solution's surface tension, which is one of the features of a surfactant, in the general sense of this term.[10] On the other hand, DDB is only slightly amphiphilic, insofar as the benzene nucleus is "more hydrophilic" than the paraffin chain: the interfacial tensions of benzene and *n*-dodecane against water are 35.0 and 52.2 mN/m, respectively, at 20 °C.[11,12] Still, DDB possesses two of the major properties of a surfactant: it adsorbs at the air−water interface and markedly lowers the surface tension. For this reason DDB could be called a "pseudosurfactant". In our thermodynamic modeling of adsorption, DDB is characterized with three material parameters: adsorption energy, excluded area per molecule, and a parameter for the lateral interaction in the adsorption layer. In this respect, we formally treat a pseudosurfactant in the same way as a nonionic surfactant.

This paper is organized as follows. In section 2 we show how the contents of Na_2SO_4 and DDB in the used sample of DDBS can be determined by means of conductometric and surface-tension measurements. Section 3 is devoted to the theoretical interpretation of the surface tension isotherms and to the respective computational procedures. In section 4 we present numerical results about the adsorptions of DDBS and DDB and about the counterion binding, surface electric potential, Gibbs elasticity, and the effect of added NaCl. In section 5 we report that some electrolytes, like $CrCl_3$ or $Fe_2(SO_4)_3$, which release strongly binding counterions, cause a significant reduction in the surface tension even at very low bulk concentrations; the binding energies of all counterions that affect the surface tension are determined.

We hope that the developed quantitative approaches will find applications also to other surfactant−electrolyte systems. In particular, we demonstrate that a quantitative characterization of surfactant adsorption (determining the adsorption energy, excluded area per molecule, etc.) can be accomplished by determining the contents of the admixtures and accounting for their presence in the theoretical model, rather than by purifying the surfactant.

2. Experimental Section

2.1. Materials and Solutions. As mentioned above, in our experiments we used the anionic surfactant sodium dodecyl benzene sulfonate (DDBS), technical grade (Aldrich). Due to the production procedure, the sample of DDBS contained admixtures of Na_2SO_4 and unsulfonated dodecylbenzene (DDB). The concentration of Na_2SO_4 was determined by electroconductivity measurements (section 2.2), and the fraction of DDB was estimated from the experimental surface-tension isotherms (section 2.3). The atomic adsorption analysis of the used sample of technical DDBS showed that it does not contain considerable amounts of other admixtures, such as Mg, Ca, Cu, Si, Fe, Al, P, Cr, Mo, Mn, and V.

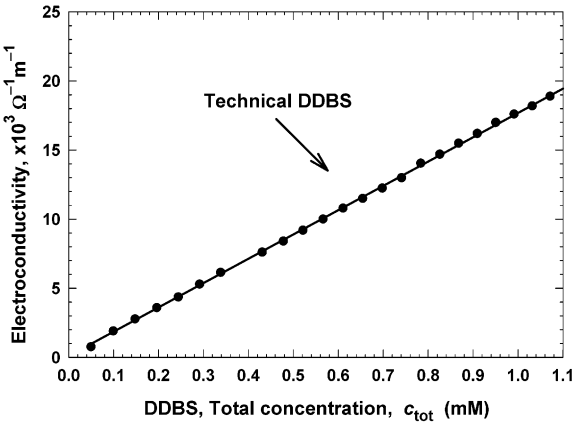

Figure 1. Electroconductivity of aqueous solutions of technical DDBS vs the total concentration c_{tot}; see eq 2.1. The experimental slope is 175.9 cm^2 Ω^{-1} mol^{-1}, and the correlation coefficient is 0.9997.

We examined experimentally the effect of added NaCl (analytical grade, Merck) on the equilibrium surface tension of the DDBS solutions. In other experiments (section 5), we investigated the influence of added minor amounts of $Fe_2(SO_4)_3 \cdot 6H_2O$ and $CrCl_3 \cdot 6H_2O$ (Sigma).

All measurements were carried out at 25 °C. The glassware was cleaned by sulfochromic acid and abundantly rinsed with deionized water from Milli-Q water purification system (Millipore Inc.). Deionized water was also used to prepare all investigated surfactant solutions.

The measurements of surface tension were carried out by means of the Wilhelmy plate method (Krüss). A commercial plate of porous platinum was used, which was cleaned before each experiment by rinsing in distilled water and heating in the flame of a spirit lamp.

The signal from the Krüss apparatus has been recorded by a computer as surface tension, σ, vs time, t. The plot of σ vs $t^{-1/2}$ exhibits a well-pronounced linear portion, which was extrapolated to $t^{-1/2} \to 0$ in order to determine the equilibrium surface tension of the respective surfactant solution.

2.2. Electroconductivity Experiments. Our electroconductivity measurements were carried out by means of a conductivity meter, model 30 (Denver Instruments, USA). Figure 1 shows the measured electroconductivity, Λ, of aqueous solutions of technical DDBS plotted vs the apparent total input concentration of DDBS, c_{tot}. The concentration c_{tot} is calculated assuming that the used surfactant sample consists of 100% DDBS.

However, as already mentioned, the sample of technical DDBS is expected to contain an admixture of Na_2SO_4. Consequently, the apparent total concentration of DDBS can be expressed in the form

$$c_{tot} = c_{DDBS} + r c_{Na_2SO_4} \tag{2.1}$$

where c_{DDBS} and $c_{Na_2SO_4}$ are the actual molar concentrations of DDBS and Na_2SO_4 and $r = M_{Na_2SO_4}/M_{DDBS} = 0.40863$ is the ratio of the molecular masses of the respective two substances. The electroconductivity of the investigated solutions of strong electrolytes is given by the relationship[13,14]

$$\Lambda = \lambda_{Na} c_{Na} + \lambda_{DDBS} c_{DDBS} + 2\lambda_{SO_4} c_{SO_4} \tag{2.2}$$

where λ_{Na} and c_{Na} are the equivalent ionic conductivity and the molar concentration of the Na^+ ions, λ_{DDBS} and c_{DDBS} are the

(10) Oldenhove de Guertechin, L. In *Handbook of Detergents, Part A*: *Properties*; Broze, G., Ed.; M. Dekker: New York, 1999; Chapter 2.
(11) Erbil, H. Y. In *Handbook of Surface and Colloid Chemistry*; Birdi, K. S., Ed.; CRC Press: Boca Raton, FL, 1997; Chapter 2.
(12) Birdi, K. S. In *Handbook of Surface and Colloid Chemistry*; Birdi, K. S., Ed.; CRC Press: Boca Raton, FL, 1997; Chapter 3.
(13) Laidler, K. J.; Meiser, J. H. *Physical Chemistry*; Houghton Mifflin Co.: Boston, 1995.
(14) Robinson, R. A.; Stokes, R. H. *Electrolyte Solutions*; Butterworth: London, 1959.

respective quantities for the $DDBS^-$ ions, and, likewise, λ_{SO_4} and c_{SO_4} refer to the SO_4^{2-} ions. Because we are dealing with relatively low ionic strengths, in eq 2.2 we have neglected the Debye–Hückel–Onsager correction factor. One can relate the actual concentrations to the input concentration, c_{tot}, as follows

$$c_{DDBS} = wc_{tot} \tag{2.3}$$

$$c_{SO_4} = c_{Na_2SO_4} = \frac{1}{r}(1 - w)c_{tot}$$

$$c_{Na} = \left[w + \frac{2}{r}(1 - w)\right]c_{tot}$$

where w is the weight fraction of DDBS contained in the technical surfactant sample. The substitution of eq 2.3 into eq 2.2 yields

$$\frac{\Lambda}{c_{tot}} = \left[w + \frac{2}{r}(1 - w)\right]\lambda_{Na} + w\lambda_{DDBS} + \frac{2}{r}(1 - w)\lambda_{SO_4} \tag{2.4}$$

The values of the equivalent ionic conductivities at 25 °C are as follows[15]

$$\lambda_{Na} = 50.1, \qquad \lambda_{SO_4} = 80.0, \qquad \lambda_{DDBS} = 28\ (cm^2\ \Omega^{-1}\ mol^{-1}) \tag{2.5}$$

The above value of λ_{DDBS} was estimated with the help of refs 14 and 16. Using the experimental value $\Lambda/c_{tot} = 175.9\ cm^2\ \Omega^{-1}\ mol^{-1}$, determined from the slope of the line in Figure 1, by means of eqs 2.4 and 2.5, we calculated the fraction of DDBS in the sample to be $w = 82.6$ wt %; correspondingly, the fraction of Na_2SO_4 is 17.4 wt %.

2.3. Surface Tension Isotherms. Figure 2 shows the obtained experimental equilibrium surface tension isotherms of DDBS for three concentrations of added NaCl: 0, 12, and 24 mM. The concentrations of DDBS correspond to the whole region below the critical micellization concentration (cmc). Along the abscissa we have plotted the actual concentration, c_{DDBS}, as determined in the previous section. The three curves corresponding to $c_{NaCl} = 0$, 12, and 24 mM are fitted simultaneously.

To fit the data we used the two-component van der Waals model, developed in part 1 of this series.[5] The three curves in Figure 2a show the *best* fit in the case when the presence of unsulfonated dodecylbenzene (DDB) is neglected in the theoretical model. In other words, to draw these curves we have assumed that the aqueous solution contains only $DDBS^-$, Na^+, Cl^-, and SO_4^{2-} ions (the content of Na_2SO_4 is as determined in section 2.2). The very poor agreement between theory and experiment in Figure 2a indicates a considerable effect of DDB on the surface tension, σ.

The three curves in Figure 2b, which excellently agree with the experimental points, represent the best fit in the case when the theoretical model accounts not only for the presence of $DDBS^-$, Na^+, Cl^-, and SO_4^{2-} ions in the solution but also for the existence of a DDB admixture in the used surfactant sample. Here we will mention in advance that the molar fraction of DDB in the mixture DDBS + DDB, determined from the fit in Figure 2b, turns out to be about 2.3 mol %, which is a quite reasonable value; see, e.g., ref 8.

Another point, which deserves a special attention is that the best fit (Figure 2b) corresponds to equal molecular excluded areas for DDBS and DDB ($\alpha_{11} = \alpha_{44}$, see ref 5). In this aspect, the situation is different from the case of the system SDS + dodecanol, where the molecular excluded areas are different for the ionic and the nonionic component ($\alpha_{11} \neq \alpha_{44}$).[5] Our result for DDBS and DDB is not surprising because the respective molecules have a benzene ring, whose diameter of 6.7 Å is greater than the diameter, 6.0 Å, of the sulfonate group.[5,17] For that reason we expect that the excluded area per DDBS and DDB molecule in a dense adsorption layer should be equal; see Figure 3. Correspondingly, to fit the experimental surface tension isotherms of DDBS, we can apply the theoretical model from section 8 of ref 9, which was derived for a mixture of an ionic and a nonionic surfactant with equal excluded areas per molecule; see eq 3.9a below. The latter model is a simpler special case of the general two-component *van der Waals* model from part 1.[5] The analogous curves, obtained by means of the *Frumkin* model, eq 3.9b below,

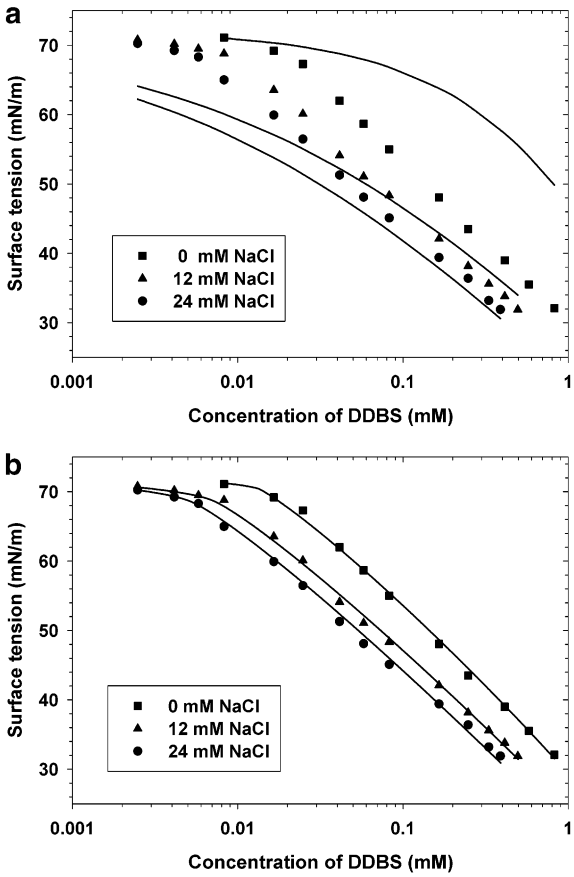

Figure 2. Plots of the surface tension, σ, vs the surfactant concentration, c_{DDBS}, for three fixed concentrations of NaCl, denoted in the figure. The curves are the best fits of the experimental points by means of the theoretical model in section 3 assuming that (a) a single anionic surfactant is present and (b) the anionic surfactant contains an admixture of nonionic surfactant, supposedly unsulfonated DDB; see Table 1 for the parameters of the best fit.

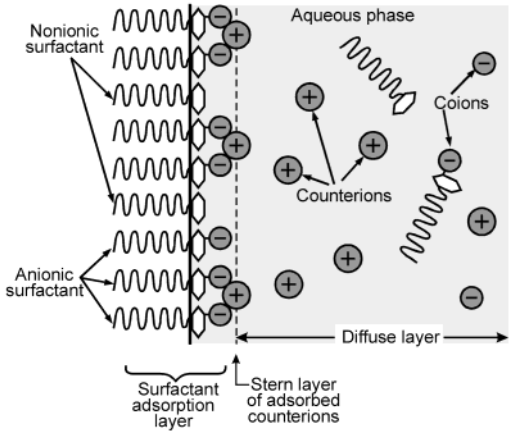

Figure 3. Sketch of the electric double layer in the vicinity of a mixed adsorption monolayer composed of DDBS and unsulfonated DDB. The Stern layer consists of adsorbed (bound) counterions, while the diffuse layer contains free ions involved in Brownian motion.

(15) Weast, R. C., Ed.; *CRC Handbook of Chemistry and Physics*; CRC Press: Boca Raton, FL, 1988.

(16) Israelachvili, J. N. *Intermolecular and Surface Forces*; Academic Press: London, 1992.

(17) Choudhary, V. R.; Nayak, V. S.; Choudhary, T. V. *Ind. Eng. Chem. Res.* **1997**, *36*, 1812.

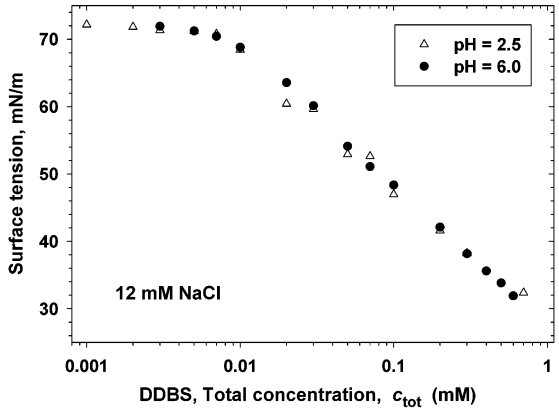

Figure 4. Plot of the surface tension, σ, vs the total concentration c_{tot}, see eq 2.1, for two fixed values of pH, 2.5 and 6.0. All solutions contain 12 mM added NaCl.

turn out to be very close to those computed using the van der Waals model, practically coinciding with them. Details about the used full set of equations, the obtained parameter values, and the computational procedure are given in section 3 below.

In principle, it is possible for the more hydrophobic DDB molecule to form a complex with the amphiphilic $DDBS^-$ ion in the bulk of solution. To check this opportunity, we tried to fit the experimental data with a model, which assumes the presence of both $DDBS^-$ monomers and $(DDB)_2S^-$ dimers in the bulk of solution. To do that we used the two-component van der Waals model from part 1.[5] The obtained best fit was poor, resembling that in Figure 2a. Hence, we may conclude that a complex $(DDB)_2S^-$ is unlikely to form in the bulk of solution. In other words, it turns out that the unsulfonated DDB behaves as a separate nonionic surfactant, as implied by the excellent fit of the data in Figure 2b; see above.

We checked experimentally the effect of lowering of pH on the equilibrium surface tension isotherm of DDBS. Figure 4 compares the isotherms of σ vs c_{DDBS} measured at pH = 6.0 and 2.5 (the latter value was adjusted by addition of HCl). One sees that there is no pronounced effect of the lowering of pH on the values of σ. One may conclude that the H^+ (or H_3O^+) ions do not exhibit a considerable (in comparison with Na^+) binding in the Stern layer. In contrast, in section 5 below it will be demonstrated that ions of Fe and Cr have a very strong effect on σ.

3. Theoretical Model

In part 1 of this study,[5] we gave a detailed description of the two-component van der Waals model. Nevertheless, in the present paper it is necessary to include an outline of the theoretical background because of the following three reasons. (i) As noted in section 2.3, for the system DDBS + DDB we can work with equal excluded areas for the two surfactant components, which leads to considerably simpler equations and computational procedure. (ii) In the present study we are dealing with asymmetric electrolytes containing divalent and trivalent ions (unlike the symmetric 1:1 electrolytes in part 1), which needs the use of some more general equations; see below. (iii) We compare fits of the surface tension isotherms by two alternative models: those of van der Waals (nonlocalized adsorption) and Frumkin (localized adsorption).[18,19]

3.1. Surface Potential and Adsorptions. In this section we describe the equations which can be used to obtain the best fit of the data in Figure 2b. In general, we are dealing with a mixed adsorption layer, composed of an ionic and a nonionic component: $DDBS^-$ and unsulfonated DDB (Figure 3). We apply the thermodynamic approach proposed in section 8 of ref 9. We will use the following numbering of the components: component 1 is $DDBS^-$, component 2 is Na^+, component 3 is Cl^-, component 4 is the unsulfonated DDB, and component 5 is SO_4^{2-}. The valence of the electric charge of the species is Z_i ($i = 1, 2, 3, ...$). The electric potential and its value at the surface are denoted by ψ and ψ_s, respectively. It is convenient to introduce also the dimensionless electric potentials

$$\Phi \equiv Z_1 e\psi/kT, \qquad \Phi_s \equiv Z_1 e\psi_s/kT \tag{3.1}$$

where e is the elementary charge, k is the Boltzmann constant, and T is the temperature. Because the $DDBS^-$ ions (component 1) determine the sign of the surface potential, both Φ and Φ_s are positive quantities. The subsurface concentration of the ith component in the solution is

$$c_{is} = c_{i\infty} \exp(-z_i\Phi_s), \qquad z_i = Z_i/Z_1 \qquad (i = 1, 2, 3, ...) \tag{3.2}$$

where $c_{i\infty}$ is the bulk concentration of this component. (For ionic strengths $\leq$0.1 M we can set the activity coefficient $\gamma_\pm \approx 1$; see ref 20.)

The surfactant adsorption isotherm, that is the relation between the subsurface concentration and the surfactant adsorption, is[9]

$$\tilde{K}_i c_{is} = \frac{\Gamma_i}{\Gamma_\infty - \Gamma} \exp\left(\frac{\eta\Gamma}{\Gamma_\infty - \Gamma} - \frac{2\beta\Gamma}{kT}\right) \qquad i = 1,\ 4 \tag{3.3}$$

where $\eta = 0$ and 1 for the Frumkin and van der Waals model, respectively, Γ_i is the surface concentration of the ith component in the surfactant adsorption monolayer, $\tilde{K}_i$ is an adsorption parameter, see eq 3.5 below, $\Gamma \equiv \Gamma_1 + \Gamma_4$ is the total *surfactant* adsorption, and Γ_∞^{-1} is the excluded area per adsorbed surfactant molecule; the interaction between such molecules is taken into account by the parameter β. The experiments with air−water and oil−water interfaces show that the value of β is dominated by the attraction between the hydrocarbon tails of the adsorbed surfactant molecules.[20,21] It is reasonable to assume that Γ_∞ and β have the same values for $DDBS^-$ and DDB. (For $\eta = 1$, eq 3.3 can be deduced as a special case of eqs 3.23 and 3.24 in ref 5 by substituting $\alpha = \alpha_{11} = \alpha_{14} = \alpha_{44} = \Gamma_\infty^{-1}, \beta_{11} = \beta_{14} = \beta_{44} = \beta, \beta_e = 0$, and by taking into account eqs 3.4 and 3.5 below.)

Since in reality the surfactant adsorption at a fluid interface is nonlocalized, in our case one may expect that the van der Waals model is more adequate than Frumkin's model. On the other hand, Frumkin's model was found to provide good fits of data for the surface tension of surfactant solutions, see, e.g., ref 3, but to predict considerably greater values for the surface elasticity than the van der Waals model.[6] To compare the two models for the system DDBS + DDB, we fitted our experimental data using alternatively the Frumkin and van der Waals models, that is, eq 3.3 for $\eta = 0$ and $\eta = 1$. The numerical results are compared and discussed in section 4.

The binding of counterions is described by the Stern isotherm;[21,22] in the present case, the surface concentration of bound Na^+ ions (component 2) per unit area of the Stern layer (Figure 3) is

$$\Gamma_2 = \Gamma_1 \frac{K_2 c_{2s}}{1 + K_2 c_{2s}} \tag{3.4}$$

(18) Frumkin, A. *Z. Phys. Chem.* **1925**, *116*, 466.
(19) Hill, T. L. *An Introduction to Statistical Thermodynamics*; Addison-Wesley: Reading, MA, 1962.

where K_2 is the adsorption parameter for the Na^+ ions in the Stern layer. The co-ions, such as Cl^- and SO_4^{2-}, are not expected to bind in the Stern layer, that is, $\Gamma_3 = \Gamma_5 = 0$. The condition for thermodynamic compatibility (see eqs 2.7 and 5.3 in ref 9) of the surfactant and counterion adsorption isotherms, eqs 3.3 and 3.4, leads to the relationship[4,9]

$$\tilde{K}_1 = K_1(1 + K_2 c_{2s}) \tag{3.5}$$

where K_1 and K_2 are constant parameters. Since DDB is treated as a nonionic surfactant, $\tilde{K}_4$ in eq 3.3 is independent of c_{2s}, that is, $\tilde{K}_4 = K_4 =$ constant. All adsorption constants K_i are related to the respective adsorption energies as follows[9]

$$K_i = \frac{\delta_i}{\Gamma_\infty} \exp\left(\frac{\Delta\mu_i^{(0)}}{kT}\right) \qquad i = 1, 2, 4, \ldots \tag{3.6}$$

Here δ_i is the thickness of the adsorption layer, which can be set equal to the characteristic dimension of the respective molecule or ion, and $\Delta\mu_i^{(0)}$ is the standard free energy of adsorption of a molecule (or ion) from an ideal dilute solution in an ideal adsorption layer (no interaction between the adsorbed species). Finally, the relationship between the surface charge and surface potential is given by the generalized Gouy equation[9]

$$\sum_i z_i\Gamma_i = \frac{2}{\kappa_c}\{\sum_i c_{i\infty}[\exp(-z_i\Phi_s) - 1]\}^{1/2} \tag{3.7}$$

where $\kappa_c^2 = (8\pi Z_1^2 e^2)/(\epsilon kT)$, with ϵ being the dielectric permittivity of water. In general, the summation in eq 3.7 is carried out over all ionic species in the solution. The left-hand side of eq 3.7 can be simplified having in mind that co-ions do not bind,[23−25] that is, $\Gamma_3 = \Gamma_5 = 0$. Note also that in our specific case $z_1 = z_3 = 1$, $z_2 = -1$, and $z_5 = 2$.

In view of eqs 3.2 and 3.5, one can consider eqs 3.3, 3.4, and 3.7 as a system of four equations for determining the four unknown variables Φ_s, Γ_1, Γ_2, and Γ_4. The numerical solution of this nonlinear system of equations is the most time-consuming step of the numerical procedure, which is described in section 3.3 below.

3.2. Calculation of the Surface Tension. The surface tension, σ, of the surfactant solution can be expressed in the form[9,26]

$$\sigma = \sigma_a + \sigma_d \tag{3.8}$$

where σ_a is the contribution of the adsorption layer, which consists of the surfactant monolayer and the counterions bound in the Stern layer (Figure 3); σ_d is the contribution of the diffuse double electric layer. For the van der Waals and Frumkin adsorption models we have, respectively[9,18,19,27,28]

$$\sigma_a = \sigma_0 - kT\Gamma/(1 - \Gamma/\Gamma_\infty) + \beta\Gamma^2 \qquad \text{(van der Waals)} \tag{3.9a}$$

$$\sigma_a = \sigma_0 + kT\Gamma_\infty \ln(1 - \Gamma/\Gamma_\infty) + \beta\Gamma^2 \qquad \text{(Frumkin)} \tag{3.9b}$$

where σ_0 is the surface tension of the pure solvent (water). Of course, it is self-consistent to use either eq 3.9a and eq 3.3 for $\eta = 1$ or eq 3.9b and eq 3.3 for $\eta = 0$. Indeed, the two equations in each couple are connected by means of the Gibbs adsorption equation,[9] $d\sigma_a = -kT\sum_i\Gamma_i\, d\ln c_{is}$.

In view of eqs 4.13 and 5.10 in ref 9, one can calculate σ_d by means of the expression

$$\sigma_d = -\frac{2kT}{\kappa_c}\int_0^{\Phi_s}\{\sum_i c_{i\infty}[\exp(-z_i\Phi) - 1]\}^{1/2}\, d\Phi \tag{3.10}$$

where the summation is carried out over all ionic species in the solution. In the case of solutions containing 1:1, 2:1, 1:2, and 2:2 electrolytes, the integral in eq 3.10 can be solved analytically; see, e.g., section 7.4 in ref 9. In a more general case, the integration in eq 3.10 can be carried out numerically.

3.3. Procedure of Data Processing. The system of equations in section 3.1 contains six unknown parameters: Γ_∞, β, K_1, K_2, K_4, and $c_{4\infty}$. The latter two parameters enter eq 3.3 only through the product $K_4c_{4\infty}$. Because component 4 is a nonionic surfactant, we have $\tilde{K}_4 = K_4$ and $c_{4s} = c_{4\infty}$. Then, the left-hand side of eq 3.3, for $i = 4$, can be expressed in the form

$$\tilde{K}_4 c_{4s} = K_4 c_{4\infty} = K_4 \frac{x_4}{1 - x_4} c_{1\infty} = \hat{K}_4 c_{1\infty} \tag{3.11}$$

where x_4 is the mole fraction of the nonionic surfactant in the investigated surfactant sample and $\hat{K}_4 = K_4x_4/(1 - x_4)$ is a new constant, which can be determined from the best fit as an adjustable parameter.

Because we do not expect a considerable difference in the binding of a Na^+ ion to a sulfate and sulfonate headgroup, in the present study we will fix the respective binding energy equal to that determined in ref 9, viz.

$$\Delta\mu_2^{(0)} = 1.64\ kT \tag{3.12}$$

Substituting the latter value in eq 3.6, one can calculate K_2 for a given Γ_∞ and for $\delta_2 \approx 0.7$ nm (the diameter of the Na^+ ion). Thus the number of the unknown parameters is reduced from 6 to 4; the latter are Γ_∞, β, K_1, and $\hat{K}_4$.

Next, we notice that the substitution of Γ_2 from eq 3.4 into eq 3.7 yields an explicit expression for Γ_1 as a function of Φ_s

$$\Gamma_1 = \frac{2}{\kappa_c}(1 + K_2c_{2s})\{\sum_i c_{i\infty}[\exp(-z_i\Phi_s) - 1]\}^{1/2} \tag{3.13}$$

see also eq 3.2. Another useful relationship is obtained by

(20) Borwankar, R. P.; Wasan, D. T. *Chem. Eng. Sci.* **1988**, *43*, 1323.
(21) Davies, J. T.; Rideal, E. K. *Interfacial Phenomena*; Academic Press: London, 1963.
(22) Stern, O., *Z. Elektrochem.* **1924**, *30*, 508.
(23) Matijevič, E.; Pethica, B. A. *Trans. Faraday Soc.* **1958**, *54*, 1382.
(24) van Voorst Vader, F. *Trans. Faraday Soc.* **1960**, *56*, 1067.
(25) Tajima, K. *Bull. Chem. Soc. Jpn.* **1971**, *44*, 1767.
(26) Hachisu, S. *J. Colloid Interface Sci.* **1970**, *33*, 445.
(27) Baret, J. F. *J. Colloid Interface Sci.* **1969**, *30*, 1.
(28) Kralchevsky, P. A.; Danov, K. D.; Denkov, N. D. In *Handbook of Surface and Colloid Chemistry*, 2nd ed.; Birdi, K. S., Ed.; CRC Press: Boca Raton, FL, 2002; Chapter 5.

summing up the equations corresponding to $i = 1$ and $i = 4$ in eq 3.3

$$[\tilde{K}_1 \exp(-\Phi_s) + \hat{K}_4]c_{1\infty} = \frac{\Gamma}{\Gamma_\infty - \Gamma} \exp\left(\frac{\eta\Gamma}{\Gamma_\infty - \Gamma} - \frac{2\beta\Gamma}{kT}\right) \tag{3.14}$$

where eq 3.11 has been used. The computational procedure is as follows:

(1) As input data we have experimental points for the interfacial tension σ at various surfactant and salt concentrations (Figure 2). Knowing c_{tot} and c_{NaCl}, one determines $c_{1\infty} = c_{DDBS}$ and $c_{5\infty} = c_{SO_4}$ with the help of eq 2.3, substituting $r = 0.40863$ and $w = 0.826$; see section 2.2. The other bulk concentrations are $c_{3\infty} = c_{NaCl}$ and $c_{2\infty} = c_{1\infty} + c_{3\infty} + 2c_{5\infty}$; $\kappa_c^2 = (8\pi Z_1^2 e^2)/(\epsilon kT)$ is a known parameter.

(2) We assign tentative values to Γ_∞, β, K_1, and $\hat{K}_4$, which are to be determined as adjustable parameters from the best fit of the data. K_2 is computed as explained after eq 3.12.

(3) We give a tentative value of the dimensionless surface potential Φ_s; a value in the interval $0 < \Phi_s < 10$ is appropriate.

(4) From eq 3.2 we calculate c_{is} for $i = 1$, 2, 3, and 5; then eq 3.5 yields $\tilde{K}_1$.

(5) From eqs 3.13 and 3.4 we calculate Γ_1 and Γ_2.

(6) Equation 3.14 is solved numerically to determine Γ; we use the bisection method. Next, we compute $\Gamma_4 = \Gamma - \Gamma_1$.

(7) The calculated values of $\Gamma_1(\Phi_s)$ and $\Gamma(\Phi_s)$ are then substituted in the equation

$$F(\Phi_s) \equiv \tilde{K}_1 \exp(-\Phi_s)c_{1\infty} - \frac{\Gamma_1}{\Gamma_\infty - \Gamma} \exp\left(\frac{\eta\Gamma}{\Gamma_\infty - \Gamma} - \frac{2\beta\Gamma}{kT}\right) = 0 \tag{3.15}$$

which is equivalent to eq 3.3 for $i = 1$. Equation 3.15 is an implicit equation for determining Φ_s, which is solved numerically; we again use the bisection method.

(8) The theoretical value of the surface tension $\sigma(c_{1\infty}^{(m)}, c_{3\infty}^{(m)}; \Gamma_\infty, \beta, K_1, \hat{K}_4)$, corresponding to a given couple of experimental concentrations of surfactant and salt ($c_{1\infty}^{(m)}$, $c_{3\infty}^{(m)}$), is then calculated from eqs 3.8−3.10.

(9) The adjustable parameters Γ_∞, β, K_1, and $\hat{K}_4$ are determined by means of the least-squares method, i.e., by numerical minimization of the merit function

$$\Psi(\Gamma_\infty, \beta, K_1, \hat{K}_4) = \left\{\frac{1}{N-1}\sum_{m=1}^{N}[\sigma^{(m)} - \sigma(c_{1\infty}^{(m)}, c_{3\infty}^{(m)}; \Gamma_\infty, \beta, K_1, \hat{K}_4)]^2\right\}^{1/2} \tag{3.16}$$

where $\sigma^{(m)}$ is the experimental value of σ, corresponding to concentrations $c_{1\infty}^{(m)}$ and $c_{3\infty}^{(m)}$, and the summation in eq 3.16 is carried out over all experimental points ($c_{1\infty}^{(m)}$, $c_{3\infty}^{(m)}$, $\sigma^{(m)}$); N is their total number.

To see how important is the effect of the unsulfonated DDB, we tried a fit (Figure 2a) assuming that such a nonionic component is absent. Then $\hat{K}_4 = 0$, $\Gamma_4 = 0$, and it is not necessary to solve eq 2.14. Hence, step 6 above must be formally replaced with $\Gamma = \Gamma_1$.

3.4. Effect of Additional Electrolytes. In some of our experiments (section 5) we added $Fe_2(SO_4)_3$ and $CrCl_3$ to the solutions of DDBS. Depending on the pH of solution, these electrolytes release monovalent, divalent, and/or trivalent counterions, for example, $Cr(OH)_2^+$, $CrOH^{2+}$, and Cr^{3+}. The above theoretical model can be upgraded to account for the presence of any additional electrolytes. In particular, the generalized form of the Stern isotherm, eq 3.4, becomes[9]

$$\frac{\Gamma_i}{\Gamma_1} = \frac{K_i c_{is}}{1 + K_2 c_{2s} + K_6 c_{6s} + K_8 c_{8s} + \cdots} \qquad i = 2, 6, 8, \ldots \tag{3.17}$$

where the even numbers $i = 6, 8, \ldots$ are chosen to denote the counterions released by the additional electrolytes, whereas the odd numbers $i = 7, 9, \ldots$ enumerate the respective co-ions. As before, it is assumed that only the counterions, but not the co-ions, can bind in the Stern layer. The generalized form of eq 3.5 is[9]

$$\tilde{K}_1 = K_1(1 + K_2 c_{2s} + K_6 c_{6s} + K_8 c_{2s} + \cdots) \tag{3.18}$$

Equation 3.6 is valid for each adsorbing species. The substitution of Γ_2, Γ_6, Γ_8, etc. from eq 3.17 into the left-hand side of eq 3.7 yields a generalized version of eq 3.13, which again expresses Γ_1 as an explicit function of Φ_s. Thus, in the presence of additional electrolytes, the computational procedure follows the same scheme, as that described in section 3.3.

4. Numerical Results and Discussion

4.1. Parameters of the Best Fit. A fit of surface tension data, like that in Figure 2b, can provide information about many properties of the interfacial layer. As already mentioned, having once determined the parameters of the fit (in our case Γ_∞, β, K_1, and $\hat{K}_4$), one is able to compute (i) the surface tension σ, (ii) the adsorptions of surfactants, Γ_1 and Γ_4, (iii) the adsorption (binding) of counterions in the Stern layer, Γ_2, and (iv) the surface electric potential ψ_s, etc., each of them for every chosen couple of surfactant and salt concentrations; see Figures 5−7. The used parameter values, corresponding to the best fit, that is, to the minimum of Ψ in eq 3.16, are listed in Table 1.

In the framework of the van der Waals model, Γ_∞^{-1} can be identified with the excluded area per molecule. Setting $\Gamma_\infty^{-1} = \pi r^2$, from the respective value in Table 1 we determine $2r = 6.7$ Å, which is exactly the outer diameter of the benzene ring, as determined by Choudhary et al.[17] in experiments on penetration of benzene molecules in zeolite channels. The latter fact is consonant with the finding that Γ_∞^{-1}, determined by means of the van der Waals model from fits of surface tension data, is equal to the geometrical cross-sectional area, πr^2, for alkanols and SDS; see Table 3 in part 1.[5] As already mentioned, the cross-sectional area of the sulfonate headgroup, 29.8 Å^2, is smaller than that of the benzene nucleus, 35.55 Å^2. This is the reason (i) the excluded area per adsorbed DDBS molecule is determined by the benzene ring and (ii) DDB and DDBS have the same excluded areas (Figure 3).

The difference between the values of Γ_∞^{-1} for the van der Waals and Frumkin models is not surprising because of the different meaning of Γ_∞^{-1} in the two models, viz., excluded area per molecule in a two-dimensional gas and area per adsorption site in a lattice, respectively.[19] For example, let us consider a dense layer of disks with square packing. If the radius of a disk is r, then the area per a square site in the lattice is $4r^2$, whereas the area of a disk is πr^2. The ratio of these areas is $4/\pi = 1.27$, which is close to the ratio of the values of Γ_∞^{-1} in Table 1, 44.0/35.5 = 1.24. However, the latter coincidence seems fortuitous,

Table 1. Parameters Determined from the Best Fits of the Data in Figure 2b

model	Γ_∞^{-1} (Å^2)	$2\beta\Gamma_\infty/kT$	K_1 (m^3/mol)	$\hat{K}_4$ (m^3/mol)	x_4 (mol %)	std dev, Ψ (mN/m)
van der Waals	35.55	6.840	248.6	5.932	2.33	0.682
Frumkin	44.00	3.985	310.6	8.454	2.65	0.690

insofar as the packing of the molecules in a dense adsorption layer is expected to be hexagonal, rather than square.[29]

The values of the dimensionless parameter $2\beta\Gamma_\infty/(kT)$ in Table 1 are close to the critical values of this parameter corresponding to the presence of a two-dimensional phase transition. (If σ_d were zero, the critical values would be $2\beta\Gamma_\infty/(kT) = 6.75$ and 4 for the van der Waals and Frumkin model, respectively.) We checked numerically that the calculated dependence of the surface pressure, $\pi_s = \sigma_0 - \sigma$, vs the area per molecule, Γ^{-1}, is a monotonic function, thanks to the contribution from the electrostatic repulsion, σ_d; see eq 3.10. In other words, for the conditions of our experiment the two adsorption layers are "supercritical," i.e., a liquid−gas phase transition in two dimensions is absent.

As in ref 9, taking $\delta_1 \approx 2$ nm and the values of K_1 and Γ_∞ in Table 1, with the help of eq 3.6, we calculate the adsorption energy per $DDBS^-$ ion: $\Delta\mu_1^{(0)}/kT = 13.27$ and 13.28 for the van der Waals and Frumkin models, respectively. In other words, the two models give practically coinciding values for $\Delta\mu_1^{(0)}$. For comparison, in the case of sodium dodecyl sulfate (SDS) we determined $\Delta\mu_1^{(0)}/kT = 12.8$; see ref 9. It is reasonable for $\Delta\mu_1^{(0)}$ to be greater for DDBS, in comparison with SDS, because DDBS has a greater hydrocarbon chain (due to the extra benzene nucleus).

As already mentioned, from the fit of the data we cannot determine separately K_4 and x_4, but only their combination $\hat{K}_4 = K_4 x_4/(1 - x_4)$. Taking approximately $\Delta\mu_4^{(0)} \approx \Delta\mu_1^{(0)}$ and $\delta_4 \approx \delta_1$, with the help of eq 3.6, we obtain $\hat{K}_4/K_1 \approx x_4/(1 - x_4)$, that is

$$x_4 \approx \frac{\hat{K}_4/K_1}{1 + \hat{K}_4/K_1} \tag{4.1}$$

The assumptions made to obtain eq 4.1 are equivalent to approximately setting $K_4 \approx K_1$. The values of the mole fraction, x_4, of the nonionic surfactant (supposedly DDB) in the sample of technical DDBS, estimated by means of eq 4.1, are given in Table 1. One sees that the van der Waals and Frumkin isotherms predict close values of x_4.

Table 1 shows also the standard deviation of the experimental points from the respective theoretical curves in Figure 2b, which is equal to the minimum value of Ψ for the respective fit; see eq 3.16. The relatively low standard deviation ($\Psi_{min} \leq 0.69$ mN/m) indicates an excellent agreement between theory and experiment. The close values of the standard deviation for the van der Waals and Frumkin models indicate that the two models provide equally good fits of the data.

4.2. Surfactant Adsorption. Figure 5a shows plots of the adsorption of $DDBS^-$, Γ_1, vs the bulk concentration of $DDBS^-$, $c_{1\infty}$, for three different fixed concentrations of added NaCl: 0, 20, and 100 mM. The curves are calculated using the system of equations described in section 3.1, substituting the parameter values from Table 1 for the two alternative models, those of van der Waals and Frumkin. For the adsorption energy of Na^+ ions, $\Delta\mu_2^{(0)}$, we always use eq 3.12. Figure 5a indicates that the adsorption of $DDBS^-$ strongly increases with the rise of the NaCl concentration. This behavior can be attributed to the reduction of the electrostatic repulsion between the $DDBS^-$ ions and the similarly charged interface due to the added electrolyte. For 20 and 100 mM NaCl, the dependence $\Gamma_1(c_{1\infty})$ exhibits a tendency to level off at higher $c_{1\infty}$. This tendency is stronger for the case of the Frumkin isotherm, although the differences between curves, computed using the two types of isotherms, are relatively

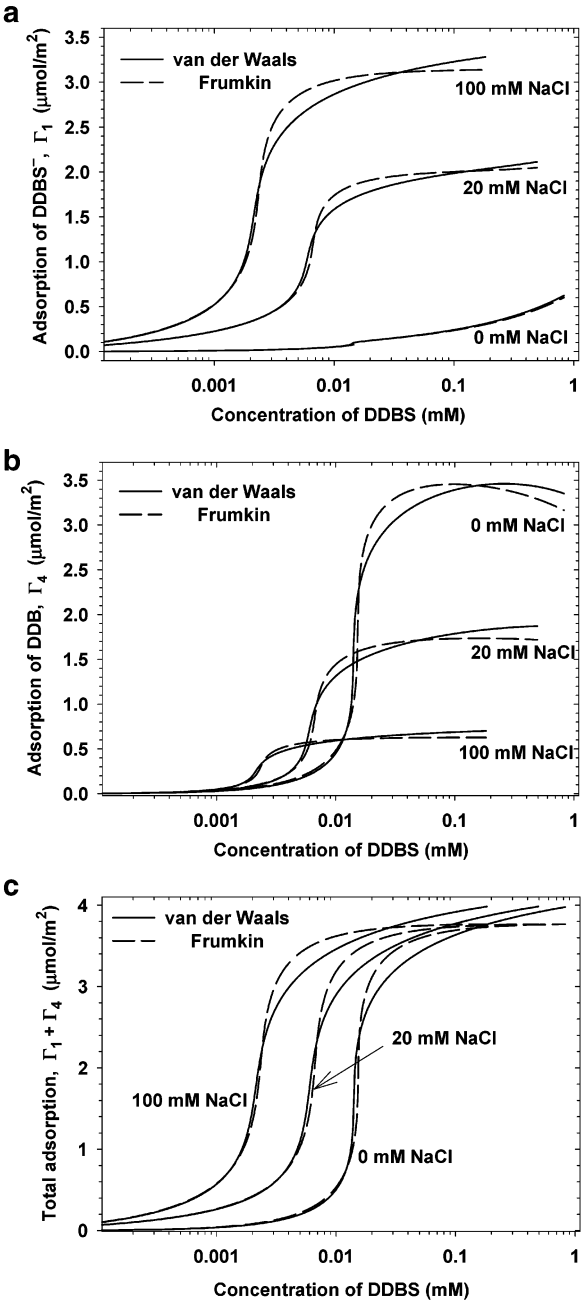

Figure 5. Plots of adsorption vs DDBS concentration, $c_{1\infty}$, calculated using the parameter values in Table 1: (a) adsorption of $DDBS^-$ ions, Γ_1; (b) adsorption of unsulfonated DDB molecules, Γ_4; (c) total surfactant adsorption, $\Gamma_1 + \Gamma_4$. The concentration of NaCl, which is fixed for each curve, is denoted in the figures.

(29) de Boer, J. H. *The Dynamical Character of Adsorption*; Clarendon Press: Oxford, 1953.

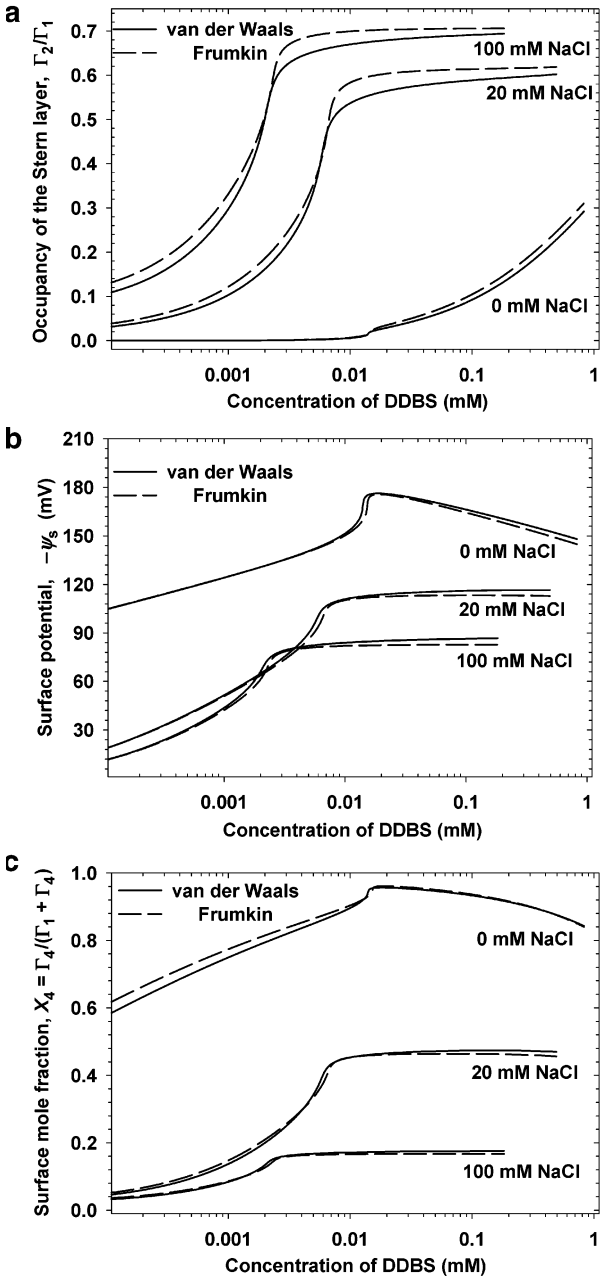

Figure 6. Plots of properties of the adsorption layer vs the DDBS concentration, $c_{1\infty}$, calculated using the parameter values in Table 1: (a) occupancy of the Stern layer, Γ_2/Γ_1; (b) negative surface potential, $-\psi_s$; (c) mole fraction, X_4, of unsulfonated DDB in the adsorption layer. The concentration of NaCl, which is fixed for each curve, is denoted in the figures.

small. Moreover, the "saturated" values of Γ_1 are different for curves with 20 and 100 mM NaCl, which can be explained with the different contents of the nonionic surfactant (supposedly unsulfonated DDB) in the adsorption layer (see Figure 5b).

The most striking result in Figure 5a is that the adsorption of $DDBS^-$ ions is rather small for the solution without NaCl (the lowest curve). The comparison with Figure 5b shows that for 0 mM NaCl the adsorption layer consists mostly of the nonionic DDB. The curves in Figure 5b indicate that the decrease in the NaCl concentration leads to an increase in the equilibrium adsorption, Γ_4, of DDB. This can be attributed to the fact that the increasing negative surface electric potential, ψ_s, repels the $DDBS^-$ ions from the subsurface zone (see Figure 6b) and they cannot compete the electroneutral DDB molecules in the adsorption at the phase boundary. In other words, for 0 mM NaCl the subsurface concentration of DDB is greater: $c_{4s} \equiv c_{4\infty} \gg c_{1s}$. For example, substituting $\psi_s = -150$ mV in eq 3.2, we get $c_{1s}/c_{1\infty} = 2.9 \times 10^{-3}$; on the other hand, $c_{4s}/c_{1\infty} \approx 2.5 \times 10^{-2}$; see the values of x_4 in Table 1. However, at a higher salt concentration, say 100 mM NaCl, the magnitude of the surface electric potential, ψ_s, is essentially reduced (Figure 6b), and the $DDBS^-$ ions, which are present at much higher bulk concentration ($c_{1\infty} \gg c_{4\infty}$), prevail in the adsorption layer: $c_{1s} > c_{4s}$, and hence $\Gamma_1 > \Gamma_4$. For example, setting $\psi_s = -90$ mV in eq 3.2, we obtain $c_{1s}/c_{1\infty} = 3.0 \times 10^{-2} > c_{4s}/c_{1\infty}$.

Figure 5c shows the total surfactant adsorption, $\Gamma = \Gamma_1 + \Gamma_4$. For each fixed NaCl concentration the isotherm Γ vs $\log(c_{1\infty})$ looks like an S-like curve. Each isotherm exhibits a portion with steepest increase (almost vertical slope), which corresponds to a certain surfactant concentration. The latter "transitional" concentration (transition from low to high surface coverage) decreases with the addition of NaCl. Although Γ_1 and Γ_4 exhibit the opposite dependencies on the NaCl concentration (Figure 5a,b), their sum, Γ, has a tendency to level off at (almost) the *same* "saturation" value, irrespective of the amount of added NaCl. Moreover, at the higher surfactant concentrations, Figure 5c indicates a pronounced difference between the $\Gamma(c_{1\infty})$-isotherms computed by means of the two alternative models: the Frumkin model predicts a faster leveling off (saturation) in comparison with the van der Waals model. This difference can be used to check which model is more adequate. For example, the curves in Figure 5c imply that at higher surfactant concentrations the Frumkin model predicts a considerably greater surface elasticity in comparison with the van der Waals model; see section 4.4.

4.3. Occupancy of the Stern Layer and Surface Mole Fraction of DDB. Figure 6a shows how the occupancy of the Stern layer, $\theta = \Gamma_2/\Gamma_1$, due to binding of Na^+ ions at the $DDBS^-$ headgroups, depends on the surfactant concentration, $c_{1\infty}$. For the two higher salt concentrations, 20 and 100 mM NaCl, θ levels off at 0.61 and 0.70, respectively. On the other hand, for 0 mM NaCl we have $\theta \leq 0.30$. Note that in the latter case the Na^+ ions originate only from the surfactant (and from the admixture of Na_2SO_4) and that the adsorption layer is composed mostly from the nonionic component (DDB); see Figure 6c. Qualitatively, the shapes of the curves $\theta(c_{1\infty})$ in Figure 6a resemble those of $\Gamma_1(c_{1\infty})$ curves in Figure 5a. Parts a and b of Figure 6 show that the Frumkin model predicts slightly greater occupancy of the Stern layer, θ, and slightly lower magnitude of the surface electric potential ψ_s, but in general, the difference between the respective curves, resulting from the two models (van der Waals and Frumkin), is small.

Figure 6b presents the dependence of the surface potential, ψ_s, on the surfactant concentration, $c_{1\infty}$. The curves at 20 and 100 mM NaCl show a monotonic increase of ψ_s with the rise of $c_{1\infty}$, followed by a leveling off at a constant value, which is, respectively, $-\psi_s \approx 115$ and 85 mV. Most interesting is the curve with 0 mM NaCl, along which $|\psi_s|$ varies from 105 to 176 mV. For this curve the adsorption, Γ_1 (Figure 5a), and the mole fraction of the ionic surfactant in the adsorption layer, $1 - X_4$ (Figure 6c), are rather low. Despite that, the magnitude of ψ_s is the highest for 0 mM NaCl. The latter effect can be explained with the lowest ionic strength, I, of the solution and with the lowest occupancy, θ, of the Stern layer in the case when the solution does not contain added NaCl. Such a behavior is predicted by the Gouy equation, eq 3.7. This

tendency is easier to be seen from the simpler form of eq 3.7 for a 1:1 electrolyte[9,21,26]

$$\sinh\left(\frac{\Phi_s}{2}\right) = \frac{\kappa_c}{4}\Gamma_1\frac{1-\theta}{I^{1/2}} \qquad (4.2)$$

see also eq 3.1. Indeed, eq 4.2 implies that smaller I and θ lead to a greater Φ_s.

The curve $|\psi_s(c_{1\infty})|$ for 0 NaCl has a maximum at $c_{1\infty} \approx$ 0.02 mM (Figure 6b). Similar nonmonotonic behavior was observed for SDS solutions.[9,20] Such a behavior can be attributed to the competition of two effects:[9] (i) the increase of the surface electric charge, $\Gamma_1(1-\theta)$, with the rise of the surfactant adsorption Γ_1 and (ii) decrease of the surface potential with the increase of the ionic strength I due to the addition ionic surfactant, which itself is an electrolyte. If there is no added NaCl, effect ii gets the upper hand at the higher $c_{1\infty}$, which explains the observed maximum. In contrast, the dependence $|\psi_s(c_{1\infty})|$ does not exhibit any maximum at 20 and 100 mM NaCl (Figure 6b) because in these cases the ionic strength is fixed by the added salt and effect ii does not appear.

Figure 6c shows the composition of the surfactant adsorption layer characterized by the surface mole fraction of the nonionic component: $X_4 = \Gamma_4/(\Gamma_1 + \Gamma_4)$. In shape, the curves in Figure 6c resemble those in Figure 6b, which is evidence for a pronounced correlation between the surface electric potential ψ_s and the surface composition X_4. An impressive fact is that the surface fraction of the nonionic component varies from $X_4 \approx 0.60$ to 0.96 in the case without NaCl, having in mind that the *bulk* fraction of the same component in the surfactant blend is only $x_4 \approx 0.025$; see Table 1. With the rise of the salt concentration, the fraction of the adsorbed nonionic decreases: its maximum values are $X_4 \approx 0.47$ and 0.17 for 20 and 100 mM NaCl, respectively (Figure 6c).

4.4. Surface Dilatational (Gibbs) Elasticity. To calculate the surface dilatational elasticity, E_G, we used eq 4.10 in ref 5, that is

$$E_G = \frac{kT\Gamma}{(1-\Gamma/\Gamma_\infty)^{\eta+1}} - 2\beta\Gamma^2 \qquad (4.3)$$

$$\eta = 0, 1$$

where, as usual, $\Gamma = \Gamma_1 + \Gamma_4$, and $\eta = 0$ and 1, respectively, for the Frumkin and van der Waals models. Parts a and b of Figure 7 show the predictions of the latter two models for the originally used sample of DDBS with an admixture of DDB; the parameter values from Table 1 have been used. The same results for E_G are plotted in a logarithmic and linear scale in parts a and b of Figure 7, respectively, to better visualize the differences between the two models at the lower and higher DDBS concentrations.

First of all, one sees a significant difference between the van der Waals and Frumkin models: the latter predicts much greater values of E_G at the higher surfactant concentration, including values $E_G \geq 2000$ mN/m. On the other hand, E_G predicted by the van der Waals model never exceeds 500 mN/m (Figure 7a,b). A similar difference between the two models was established in ref 6 for solutions of SDS. To find which of the two models is more realistic, their predictions can be compared with the experimentally measured surface elasticity at concentrations just below the cmc. This could be a subject of a subsequent study. Our expectation is that the van der Waals model should be more adequate, insofar as it is based on the assumption for nonlocalized adsorption, which is the case of surfactant adsorption at a fluid

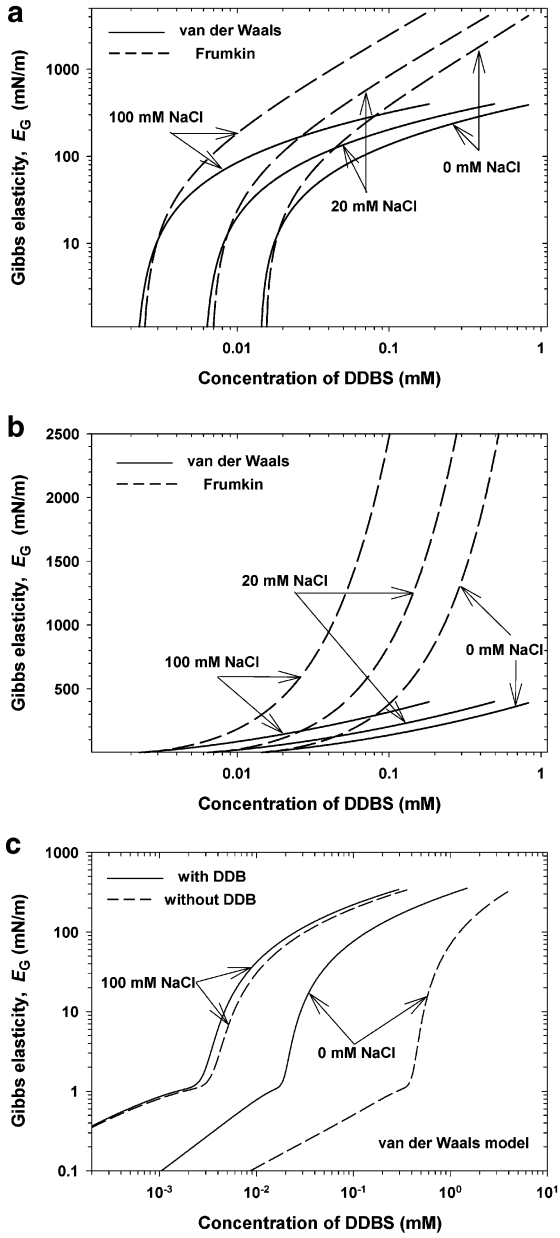

Figure 7. Plots of the surface dilatational (Gibbs) elasticity, E_G, vs the DDBS concentration, $c_{1\infty}$, calculated using the parameter values in Table 1: (a) comparison of the van der Waals and Frumkin models for three salt concentrations denoted in the figure; (b) the same as in (a) but with a linear scale along the ordinate; (c) comparison of curves calculated by using the van der Waals model, assuming absence and presence of DDB, respectively $x_4 = 0$ and 2.33 mol %.

interface. Quantitatively, this results in physically relevant values of Γ_∞ determined by the van der Waals fits; see section 4.1. One of the reasons for the considerably greater E_G predicted by the Frumkin model is the smaller value of Γ_∞ for this model (Table 1), which leads to larger E_G when substituted in the denominator of eq 4.3.

Second, parts a and b of Figure 7 show a strong increase of E_G with the rise of the NaCl concentration. This result can be explained with the greater total adsorption, $\Gamma = \Gamma_1 + \Gamma_4$, at a higher NaCl concentration; see Figure 5c and eq 4.3.

A third significant effect is illustrated in Figure 7c; this is the effect of the nonionic admixture (DDB) on the surface elasticity. In this figure, we compare the theoretical curves, predicted by the van der Waals model, for mole fractions of DDB $x_4 = 0$ and 2.33 mol % (in the surfactant blend),

all other parameters of the system being the same. For solutions without added NaCl, the effect of DDB is tremendous: E_G is greater by orders of magnitude for the solution with $x_4 = 2.33$ mol % DDB. On the other hand, at a high ionic strength, 100 mM NaCl, the effect of DDB on the Gibbs elasticity, E_G, becomes small; see the upper two curves in Figure 7c. The latter results are related to the fact that at high ionic strengths DDBS displaces DDB from the adsorption layer; see Figures 5 and 6c.

It is known that at greater Gibbs elasticity the liquid films, the foams and the emulsions are more stable.[30] A practical implication from Figure 7c is that it is sufficient to add a small fraction of a nonionic surfactant to an ionic one, to strongly increase the surface elasticity and to achieve a greater stability of liquid films and fluid dispersions.

5. Solutions with $CrCl_3$ and $Fe_2(SO_4)_3$

The addition of a sufficiently high amount of $CrCl_3$ or $Fe_2(SO_4)_3$ to a water solution of an anionic surfactant, such as SDS and DDBS, leads to precipitation. In other words, such salts interact more strongly with the surfactant than the NaCl. Then, we may expect that even a small amount of dissolved $CrCl_3$ or $Fe_2(SO_4)_3$, which does not yet cause precipitation, will have a strong impact on the surface tension of the anionic surfactant solution. To check the latter hypothesis we carried out the following experiments.

5.1. Solutions with $CrCl_3$. We measured the dependence of the surface tension, σ, on the concentration of dissolved $CrCl_3$ at a fixed concentration of technical DDBS, viz., $c_{tot} = 50\ \mu$M ($c_{DDBS} = 41.3\ \mu$M); see eq 2.1. In one set of experiments the pH had its *natural* (self-adjusted) value, determined by the input concentration of $CrCl_3$; in these experiments pH varied with C_{CrCl_3}. In another set of experiments, we fixed pH = 6 by adding an appropriate amount of NaOH to the solution. The experimental data for σ vs C_{CrCl_3} are plotted in Figure 8a, where the values of the self-adjusted pH are shown for each concentration of $CrCl_3$.

The type of ions in the investigated solutions of $CrCl_3$ depends on pH. The equilibrium constants of dissociation of the various ionic species, defined by the relationships

$$k_1 \equiv \frac{[CrOH^{2+}]}{[Cr^{3+}][OH^-]} \qquad (5.1)$$

$$k_{1,2} \equiv \frac{[Cr(OH)_2{}^+]}{[Cr^{3+}][OH^-]^2}$$

$$k_{1,2,3} \equiv \frac{[Cr(OH)_3]}{[Cr^{3+}][OH^-]^3}$$

are $\log(k_1) = 10.0$, $\log(k_{1,2}) = 18.3$, and $\log(k_{1,2,3}) = 24.0$; see ref 31. With the help of eq 5.1, we obtain expressions for the concentrations of the different ions at a given pH

$$[CrOH^{2+}]/[Cr^{3+}] = 10^{pH-4} \qquad (5.2)$$

$$[Cr(OH)_2{}^+]/[CrOH^{2+}] = 10^{pH-5.7}$$

$$[Cr(OH)_3]/[Cr(OH)_2{}^+] = 10^{pH-8.3}$$

Using eq 5.2, we computed the mole fractions of the chromium-containing species for the experimental pH values shown in Figure 8a; the results are listed in Table 2. One sees that the fraction of $Cr(OH)_3$ is always negligible and that Cr^{3+} could have a slight effect only at the lowest experimental pH. In this range of pH values the dissolving of $CrCl_3$ results mostly in the appearance of $Cr(OH)_2{}^+$ and $CrOH^{2+}$ ions in the solution.

The theoretical fits in Figure 8a are drawn as explained in section 3.4 above. In particular, the parameters Γ_∞, β, K_1, and $\hat{K}_4$ have been already determined from the fit of the data in Figure 2b. We used the van der Waals model and the respective values of Γ_∞, β, K_1, and $\hat{K}_4$ given in Table 1. The binding of the chromium ions in the Stern layer is described by eq 3.17, with K_6, K_8, and K_{10} denoting the adsorption constants of the $Cr(OH)_2{}^+$, $CrOH^{2+}$, and Cr^{3+} ions, respectively. All experimental points in Figure 8a were processed simultaneously with the theoretical model using K_6, K_8, and K_{10} as adjustable parameters. It turns out that because of the low molar fraction of Cr^{3+}, the fit is not sensitive to the value of K_{10}, which therefore

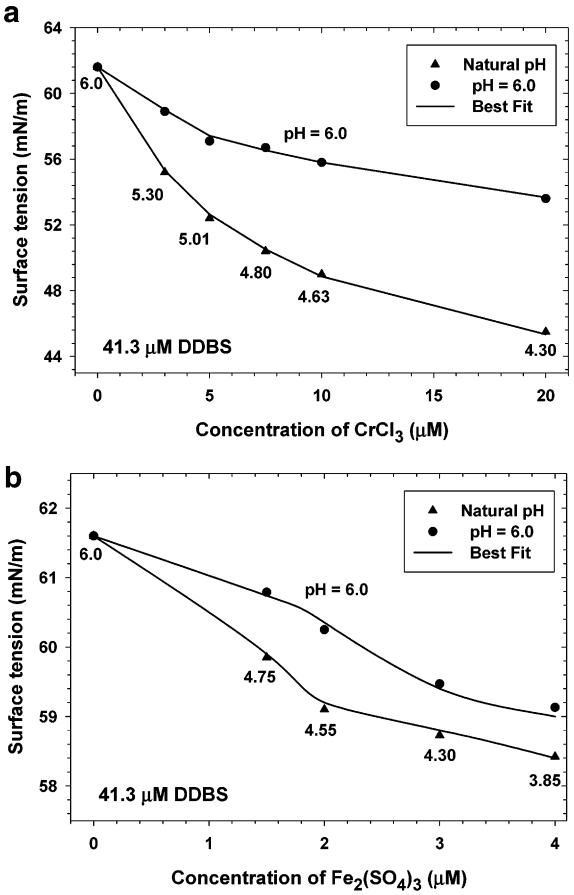

Figure 8. Surface tension, σ, of aqueous solutions of DDBS vs the concentration of added inorganic electrolyte: (a) $CrCl_3$; (b) $Fe_2(SO4)_3$. The concentration of DDBS is fixed at 41.3 μM. The lower curve corresponds to the natural (self-adjusted) values of pH, which are denoted in the figure. The upper curve is obtained at pH = 6.0, which has been adjusted constant by the addition of NaOH.

Table 2. Mole Fractions of the Cr Components in Aqueous Solutions at Various pH

pH	$[Cr(OH)_3]$	$[Cr(OH)_2{}^+]$	$[CrOH^{2+}]$	$[Cr^{3+}]$
4.30	2.58×10^{-6}	2.58×10^{-2}	6.49×10^{-1}	3.25×10^{-1}
4.63	1.38×10^{-6}	6.45×10^{-2}	7.58×10^{-1}	1.78×10^{-1}
4.80	3.10×10^{-5}	9.80×10^{-2}	7.79×10^{-1}	1.23×10^{-1}
5.01	8.04×10^{-5}	1.57×10^{-1}	7.68×10^{-1}	7.51×10^{-2}
5.30	2.75×10^{-4}	2.75×10^{-1}	6.90×10^{-1}	3.46×10^{-2}
6.00	3.32×10^{-3}	6.62×10^{-1}	3.32×10^{-1}	3.32×10^{-3}

(30) Ivanov, I. B.; Kralchevsky, P. A. *Colloids Surf., A* **1997**, *128*, 155.

(31) Lurye, Y. Y. *Handbook of Analytical Chemistry*; Chemistry: Moscow, 1989 (Russian).

Table 3. Mole Fractions of the Fe Components in Aqueous Solutions at Various pH

pH	$[Fe(OH)_3]$	$[Fe(OH)_2^+]$	$[FeOH^{2+}]$	$[Fe^{3+}]$
3.85	2.32×10^{-3}	6.70×10^{-1}	2.92×10^{-1}	6.53×10^{-3}
4.30	8.06×10^{-3}	8.63×10^{-1}	1.28×10^{-1}	1.01×10^{-3}
4.55	1.51×10^{-2}	9.09×10^{-1}	7.56×10^{-2}	3.38×10^{-4}
4.75	2.44×10^{-2}	9.27×10^{-1}	4.86×10^{-2}	1.37×10^{-4}
6.00	3.18×10^{-1}	6.80×10^{-1}	2.01×10^{-3}	3.18×10^{-7}

cannot be determined as an adjustable parameter from the considered set of data. Thus, in fact we have only two adjustable parameters; their values, determined from the best fit, are $K_6 = 1.161$ m^3/mol and $K_8 = 5.117 \times 10^{-3}$ m^3/mol. Next, with the help of eq 3.6 we determine the standard adsorption energies: $\Delta\mu_{Cr(OH)_2^+}^{(0)} = 8.60\ kT$ and $\Delta\mu_{CrOH^{2+}}^{(0)} = 3.17\ kT$. A discussion about the latter values, in comparison with the adsorption energies of other counterions, is given in section 5.3 below.

It should be noted that the standard deviation of the fit of the data in Figure 8a is $\Psi_{min} = 0.23$ mN/m, see eq 3.16, which means that the agreement between theory and experiment is excellent. The calculated theoretical points practically coincide with the experimental ones. The curves in Figure 8a represent spline lines passing through the theoretical points.

5.2. Solutions with $Fe_2(SO_4)_3$. We measured also the dependence of the equilibrium surface tension, σ, on the concentration of dissolved $Fe_2(SO_4)_3$ at the same fixed concentration of technical DDBS as in section 5.1, viz., $c_{tot} = 50\ \mu$M ($c_{DDBS} = 41.3\ \mu$M); see eq 2.1. Again, in one set of experiments the pH had its *natural* (self-adjusted) value determined by the input concentration of $Fe_2(SO_4)_3$. In another set of experiments we fixed pH = 6 by addition of NaOH. The experimental data for σ vs $C_{Fe_2(SO_4)_3}$ are plotted in Figure 8b, where the values of the natural pH at each concentration of $Fe_2(SO_4)_3$ are shown.

The type of ions in the investigated solutions of $Fe_2(SO_4)_3$ depends on pH. The equilibrium constants of dissociation of the various ionic species, defined by the relationships

$$k_1 \equiv \frac{[FeOH^{2+}]}{[Fe^{3+}][OH^-]} \tag{5.3}$$

$$k_{1,2} \equiv \frac{[Fe(OH)_2^+]}{[Fe^{3+}][OH^-]^2}$$

$$k_{1,2,3} \equiv \frac{[Fe(OH)_3]}{[Fe^{3+}][OH^-]^3}$$

are $\log(k_1) = 11.8$, $\log(k_{1,2}) = 22.33$, and $\log(k_{1,2,3}) = 30.0$; see ref 31. With the help of eq 5.3 we obtain expressions for the concentrations of the different ions at a given pH

$$[FeOH^{2+}]/[Fe^{3+}] = 10^{pH-2.2} \tag{5.4}$$

$$[Fe(OH)_2^+]/[FeOH^{2+}] = 10^{pH-3.47}$$

$$[Fe(OH)_3]/[Fe(OH)_2^+] = 10^{pH-6.33}$$

Using eq 5.4, we computed the mole fractions of the iron-containing species for the experimental pH values shown in Figure 8b; the results are listed in Table 3. One sees that the fraction of $Fe(OH)_2^+$ is always predominant, while the fraction of Fe^{3+} is always negligible.

The theoretical fits in Figure 8b are drawn as explained in section 3.4 above. We used the van der Waals model and the respective values of Γ_∞, β, K_1, and $\hat{K}_4$ given in Table 1. The binding of the iron ions in the Stern layer is described by eq 3.17, with K_6, K_8, and K_{10} denoting the adsorption constants of the $Fe(OH)_2^+$, $FeOH^{2+}$, and Fe^{3+} ions, respectively. All experimental points in Figure 8b were processed simultaneously with the theoretical model using K_6, K_8, and K_{10} as adjustable parameters. It turns out that because of the low molar fraction of the $FeOH^{2+}$ and Fe^{3+} ions, the fit is not sensitive to the values of K_8 and K_{10}, which therefore cannot be determined as adjustable parameters from the considered set of data. Thus, in fact we have only one adjustable parameter; its value determined from the best fit is $K_6 = 1.919$ m^3/mol. Next, with the help of eq 3.6 we determine the respective standard adsorption energy: $\Delta\mu_{Fe(OH)_2^+}^{(0)} = 9.10\ kT$. A discussion about the latter value, in comparison with the adsorption energies of other counterions, is given in the next section.

The standard deviation of the fit of the data in Figure 8b is $\Psi_{min} = 0.26$ mN/m, see eq 3.16, which means that again we have an excellent agreement between theory and experiment. The calculated theoretical points practically coincide with the experimental ones. The curves in Figure 8b represent spline lines passing through the theoretical points.

Table 4. Binding Energies of Counterions at Sulfonate Headgroups

counterion	$\Delta\mu_i^{(0)}/kT$
Na^+	1.64
$CrOH^{2+}$	3.17
$Cr(OH)_2^+$	8.60
$Fe(OH)_2^+$	9.10

5.3. Discussion. Table 4 compares the values of the standard adsorption energies, $\Delta\mu_i^{(0)}$ of the counterions in the Stern layer. We recall that $\Delta\mu_i^{(0)}$ was determined from the fits of experimental data about the effect of the respective electrolytes on the surface tension of anionic surfactant solutions; see eqs 3.6 and 3.12 and sections 5.1 and 5.2.

As mentioned in relation to eq 3.12, from a viewpoint of molecular structure we expect the counterion binding energies, $\Delta\mu_i^{(0)}$, to be practically the same for surfactants with sulfonate and sulfate headgroups. Moreover, the value $\Delta\mu_i^{(0)} = 1.64\ kT$ for the binding of Na^+ counterions to a planar adsorption layer is very close to the values $\Delta\mu_i^{(0)} = 1.4-1.6\ kT$ for the energy of binding of Na^+ ions to the surface of cylindrical anionic micelles; see Table 1 in ref 32. Hence, we can attribute $\Delta\mu_i^{(0)}$ for Na^+ to an excess electrostatic interaction (per counterion) due to the *discreteness* of the surface electric charge; see eq 3.28 and Figure 7 in ref 32. Note that this excess electrostatic interaction is proportional to the counterion valence. Because we have $\Delta\mu_{CrOH^{2+}}^{(0)} = 3.17\ kT \approx 2\Delta\mu_{Na^+}^{(0)}$, one could attribute the binding energy of the $CrOH^{2+}$ ions again to the discreteness of the surface electric charge. On the other hand, $\Delta\mu_i^{(0)}$ is considerably larger, about 9 kT, for the doubly hydrated $Cr(OH)_2^+$ and $Fe(OH)_2^+$ ions, which cannot be interpreted as a simple electrostatic effect (otherwise these monovalent counterions would have adsorption energy close to that of Na^+). One could hypothesize that the OH groups of $Cr(OH)_2^+$ and $Fe(OH)_2^+$ interact specifically with the sulfate anion and probably take part in its hydration shell, which could contribute to greater binding energies of these counterions (Table 4).

(32) Alargova, R. G.; Danov, K. D.; Kralchevsky, P. A.; Broze, G.; Mehreteab, A. *Langmuir* **1998**, *14*, 4036.

6. Summary and Conclusions

By means of the Wilhelmy plate method, equilibrium surface tension isotherms of DDBS are obtained for surfactant concentrations below the cmc and for 0, 12, and 24 mM added NaCl and pH = 6. The used technical DDBS contains admixtures of Na_2SO_4 and unsulfonated DDB. The content of Na_2SO_4 is found by electroconductivity measurements (Figure 1), whereas the content of DDB is determined by processing the surface-tension data; see Figure 2 and Table 1. In particular, to estimate the fraction, x_4, of DDB in the used DDBS sample, we employed the approximation $K_4 \approx K_1$ and obtained $x_4 = 2.33$ mol % (Table 1).

Having once determined the parameters of the best fit (Γ_∞, β, K_1, and $\hat{K}_4$), we are able to compute the surface tension, σ, the adsorptions of surfactants, Γ_1 and Γ_4, the adsorption (binding) of counterions in the Stern layer, Γ_2, the surface electric potential ψ_s, the surface elasticity, E_G, etc., each of them for every chosen couple of surfactant and salt concentrations; see Figures 5−7. To interpret the data we used two alternative models: those of van der Waals and Frumkin. The two models give equally good fits of the data (Table 1) and close predictions about some properties of the adsorption layer (Figures 5 and 6) but very different predictions about the surface elasticity (Figure 7a,b). The van der Waals model seems more adequate because it gives an excluded area per DDBS molecule, Γ_∞^{-1}, exactly equal to the cross-sectional area of the benzene ring, $\pi r^2 = 35.6$ Å^2 (section 4.1), which results in moderate values of the surface elasticity at the higher surfactant concentrations (eq 4.3 and Figure 7).

The adsorption of $DDBS^-$ ions, Γ_1, strongly increases with the rise of the NaCl concentration (Figure 5a). A striking result is that Γ_1 is rather low for the solution without added NaCl: in this case the adsorption layer consists mostly of the nonionic DDB, irrespective of its small mole fraction in the surfactant blend (Figure 5a,b). This result is attributed to the fact that the increasing negative surface electric potential, ψ_s (Figure 6b), repels the $DDBS^-$ ions from the subsurface zone and they cannot compete the electroneutral DDB molecules in the adsorption at the phase boundary. The rise of the total surfactant adsorption, $\Gamma = \Gamma_1 + \Gamma_4$, due to the presence of a small amount of DDB, results in a considerable increase of the surface elasticity, E_G; see Figure 7c.

The occupancy of the Stern layer, $\theta = \Gamma_2/\Gamma_1$, due to binding of Na^+ ions at the headgroups of $DDBS^-$, depends on the surfactant concentration. For the two higher salt concentrations, 20 and 100 mM NaCl, θ levels off at 0.61 and 0.70, respectively (Figure 6a). This comparatively high occupancy is in line with the results of other studies.[9] On the other hand, for 0 mM NaCl we have a relatively low occupancy, $\theta \leq 0.30$. In the latter case the adsorption layer is composed mostly (up to 96%) from the nonionic component (DDB); see Figure 6c. Despite that, the magnitude of the surface electric potential is the highest for 0 mM NaCl. This finding can be explained with the lowest solutions' ionic strength and the lowest occupancy of the Stern layer in the case without NaCl; see eq 4.2.

The comparison of surface tension isotherms obtained at pH = 2.5 and 6.0 shows no indications about the binding of H^+ ions (Figure 4). In contrast, even minimal added amounts (micromoles) of $CrCl_3$ or $Fe_2(SO_4)_3$ cause a significant reduction in the surface tension (Figure 8). The theoretical analysis of this effect allowed us to determine the adsorption energies of the $CrOH^{2+}$, $Cr(OH)_2^+$, and $Fe(OH)_2^+$ ions in the Stern layer (Table 4). There are indications that the binding of Na^+ and $CrOH^{2+}$ ions is due mostly to excess electrostatic interactions, whereas the $Cr(OH)_2^+$ and $Fe(OH)_2^+$ ions exhibit some specific interactions with the sulfonate (or sulfate) headgroups of the adsorbed surfactant molecules, which leads to a markedly larger binding energy of these doubly hydrated counterions (Table 4).

In summary, the present paper gives an example for a detailed analysis of aqueous solutions of a technical ionic surfactant. The admixtures of electrolyte and nonionic surfactant in the used sample are determined; the surface tension data are interpreted by means of a theoretical model; the equilibrium properties of the surfactant adsorption layer are quantified, and the binding energies of various counterions are determined. Using the obtained parameter values (Table 1), and the developed computer program (section 3.3), one can further predict (i) the dynamic behavior of the surface tension and (ii) the equilibrium thickness and other properties of foam films formed from solutions of the investigated surfactant; this could be a subject of subsequent studies.

Our major result is the demonstration that the presence of a DDB admixture in DDBS can have considerable consequences in several aspects: pronounced decrease of the surface tension of DDBS aqueous solutions (Figure 2); significant molar fraction of DDB in the adsorption layer (Figure 6c); strong increase in the surface dilatational elasticity (Figure 7c); displacement of DDB from the adsorption layer by addition of NaCl (Figure 5b). We hope that the reported results could provoke interest and promote future studies in this field. The latter might include obtaining of chemically pure DDBS (which is not commercially available now) and verification of the theoretical predictions in the present article, which are based on an analysis of data for a technical-grade DDBS. In other words, the experimental verification of the model by mixing of pure components (DDBS and DDB) remains to be done.

Acknowledgment. This work was supported by Colgate-Palmolive. The authors are indebted to Professor Ivan B. Ivanov and Professor Nikolai D. Denkov for the helpful discussions.

LA0268505